FORMATION OF NITROGEN AND HYDROGEN-BEARING MOLECULES IN SOLID AMMONIA AND IMPLICATIONS FOR SOLAR SYSTEM AND INTERSTELLAR ICES

Weijun Zheng,[1,2] David Jewitt,[1] Yoshihiro Osamura,[3] and Ralf I. Kaiser[2]

ABSTRACT

We irradiated solid ammonia (NH_3) in the temperature range of 10–60 K with high-energy electrons to simulate the processing of ammonia-bearing ices in the interstellar medium and in the solar system. By monitoring the newly formed molecules *online* and *in situ*, the synthesis of hydrazine (N_2H_4), diazene (N_2H_2 isomers), hydrogen azide (HN_3), the amino radical (NH_2), molecular hydrogen (H_2), and molecular nitrogen (N_2) has been confirmed. Our results show that the production rates of hydrazine, diazene, hydrogen azide, molecular hydrogen, and molecular nitrogen are higher in amorphous ammonia than those in crystalline ammonia; this behavior is similar to the production of molecular hydrogen, molecular oxygen, and hydrogen peroxide found in electron-irradiated water ices. However, the formation of hydrazine in crystalline ammonia does not show any temperature dependence. Our experimental results give hints to the origin of molecular nitrogen in the Saturnian system and possibly in the atmospheres of proto-Earth and Titan; our research may also guide the search of hitherto unobserved nitrogen-bearing molecules in the interstellar medium and in our solar system.

Subject headings: astrobiology — astrochemistry — cosmic rays — infrared: general — methods: laboratory — planets and satellites: general

Online material: color figures

1. INTRODUCTION

Ammonia is not only a building block of biologically important molecules such as amino acids and proteins, but also a valuable condensable species in the solar system (Sill et al. 1980). Ammonia and/or ammonia hydrate has been found in the atmospheres of Jupiter (Atreya et al. 2003), Saturn (Atreya et al. 2003), Uranus (Hofstadter & Muhleman 1989), and Neptune (Lindal 1992), as well as on the surfaces of their icy satellites such as Miranda, Mimas, Enceladus, Tethys, and Rhea (Bauer et al. 2002; Emery et al. 2005). The existence of ammonia hydrates on Kuiper Belt objects has been reported (Jewitt & Luu 2004). Ammonia has also been identified in the dust grains in cold molecular clouds with an abundance of 1%–10% with respect to water (Greenberg et al. 1983; Maret et al. 2006). The abundance of ammonia in the ices of comets and protostars is lower than water (H_2O), carbon monoxide (CO), and carbon dioxide (CO_2), but higher than methane (CH_4; Roush 2001). The ices in these cold molecular clouds and on solar system bodies are subjected to the irradiation by cosmic-ray particles (Cesarsky & Volk 1978; Clayton & Jin 1995), UV photons (Cecchi-Pestellini et al. 1995), the solar wind (Cooper et al. 2003), or by energetic particles trapped in planetary magnetospheres (Cooper et al. 2001). Therefore, the understanding of the processing of solid ammonia by ionizing particles and ultraviolet photons is important for a detailed understanding of the chemical evolution of cold molecular clouds and of our solar system. We recognize that ammonia is hardly a pure ice, but mixed with species such as water. Therefore, it is essential to study the mixtures of ammonia with various molecules under realistic conditions. However, in order to understand the chemical processes in complex mixtures, we first need to gain a detailed knowledge on the irradiation products and chemical processing of ammonia.

Several previous laboratory experiments have been conducted to study the effects of energetic particles and photons on solid ammonia. Haring et al. (1983) and De Vries et al. (1984) investigated the sputtering of solid ammonia with 3 keV Ar^+ and He^+. They detected the formation of hydrazine (N_2H_4) and molecular nitrogen (N_2). Johnson et al. (1983) probed the sputtering of solid ammonia with 1.5 MeV He^+. A UV photon processing of solid ammonia was conducted by Gerakines et al. (1996) and the infrared absorption features of newly formed hydrazine (N_2H_4), the amino radical (NH_2), and molecular hydrogen (H_2) were reported. Very recently, it has been shown that the impact of ^{252}Cf fission fragments on solid ammonia produced negative clusters of the series $(NH_3)_nNH_2^-$ and $(NH_3)_nNH_4^+$ (Farenzena et al. 2005). Note that in addition to the astrophysical importance of solid ammonia, the effect of irradiation on solid ammonia is also interesting from the chemical viewpoint. The spectroscopic properties and reactivity of ammonia and its derivatives such as hydrazine (N_2H_4) and diazene (N_2H_2) have been investigated with a variety of methods, such as photodesorption (Szulczewski & White 1998), matrix isolation (Catalano et al. 1963; Rosengren & Pimentel 1965), and theoretical calculations (Pople & Curtiss 1991; Durig & Zheng 2002; Hwang & Mebel 2003; Biczysko et al. 2006; Matus et al. 2006). In the present work, we conduct a detailed experimental investigation of the chemical processing of ammonia ices over a broad temperature range (10–60 K) by energetic electrons to simulate the effects of secondary electrons; the latter are either generated in the track of Galactic cosmic-ray particles or can be trapped in the magnetospheres of the giant planets. We also probe the dependence of the reaction mechanisms and the yields on the morphology of the ammonic samples, i.e., crystalline versus amorphous.

2. EXPERIMENTAL

The experiments were carried out in an ultra–high-vacuum chamber (Bennett et al. 2004). Briefly, a two-stage closed-cycle helium refrigerator coupled with a rotary platform is attached to

[1] Institute for Astronomy, University of Hawaii–Manoa, Honolulu, HI 96822.
[2] Department of Chemistry, University of Hawaii–Manoa, Honolulu, HI 96822; ralfk@hawaii.edu.
[3] Department of Chemistry, Rikkyo University, Tokyo, 171-8501, Japan.

the main chamber and holds a polished polycrystalline silver mirror serving as a substrate for the ice condensation. With the combination of the closed-cycle helium refrigerator and a programmable temperature controller, the temperature of the silver mirror can be regulated precisely to ± 0.3 K between 10 and 350 K. The amorphous ammonia was prepared by condensing anhydrous ammonia (99.99%; Matheson Gas Products, Inc.) onto the silver mirror at 10 K. Cubic crystalline ammonia ice was prepared by warming up the amorphous ammonia to 84 K (Zheng & Kaiser 2007) at a speed of 0.5 K minute^{-1} followed by a cooling to the desired temperatures (10, 40, and 60 K). The gas lines and the gas reservoir were baked and pumped down to 2×10^{-7} torr for several hours to eliminate possible contamination from water molecules and air. The background pressure in the main chamber, in which the sample was deposited, was 7×10^{-11} torr. During the condensation, the capillary array was located 0.5 cm from the silver mirror; the pressure of the ammonia in the main chamber was maintained at 5.0×10^{-9} torr for about 5 minutes and 20 s. The thickness of the ammonia ices formed on the silver mirror was estimated to be about 135 ± 30 nm based on the integrated infrared absorption coefficient of the 3 μm (3000–3700 cm^{-1}) band $A_{\text{ref}}(3000{-}3700 \text{ cm}^{-1}) = 1.03 \times 10^6$ cm^{-2} (Sill et al. 1980) and a modified Lambert-Beer relationship (Bennett et al. 2004). The variations of the thickness in our experiments were less than 5% from day to day. However, we would like to point out that the accuracy of the absolute thickness depends on the accuracy of the absorption coefficient given in the literature.

In our experiments, the samples were irradiated with 5 keV electrons for 180 minutes at electron currents of 0 (blank experiment) or 100 nA by scanning the electron beam over an area of 1.86 ± 0.02 cm^2. The pressure in the main chamber was about $(6{-}9) \times 10^{-11}$ torr during the irradiation. After each irradiation, the samples were kept at the same temperature for 60 minutes and were then warmed up at the speed of 0.5 K minute^{-1} until the molecules have sublimed. The infrared spectra of the samples were measured *online* and *in situ* by a Fourier Transform Infrared Spectrometer (Nicolet 6700 FTIR). We also used a quadrupole mass spectrometer (Balzer QMG 420) to monitor the species released to into the gas phase (mass range 1–200 amu).

3. RESULTS

3.1. *Infrared Spectra*

Figure 1 presents the infrared absorption spectra of amorphous solid ammonia before and after the irradiation at 10 K. The electron exposure triggered the appearance of new absorption features at 1514, 2088, 2348, 2805, and 3052 cm^{-1} (Table 1). The new feature at 1514 cm^{-1} can be assigned to the ν_2 bending of the amino radical (NH$_2$), that at 2088 cm^{-1} to hydrogen azide (N=N=NH; Shimanouchi 1977). It should be mentioned that the latter absorption could also originate from ammonium azide (NH$_4$N$_3$; Carlo et al. 2001). Note that Gerakines et al. (1996) observed a similar peak at 2115 cm^{-1}. The 2348 cm^{-1} absorption corresponds to newly formed molecular nitrogen (N$_2$). The broad features at 2805 and 3052 cm^{-1} can be attributed to the ν_5 mode of isodiazene (N=NH$_2$) and to the ν_5 fundamental of cis-diazene (cis-HN=NH), respectively. We did not observe the absorption features of trans-N$_2$H$_2$. It might be possible that its features are overlapping with the ammonia fundamentals; likewise, we were not able to identify the N$_2$H and N$_2$H$_3$ radicals; their absorption features overlap with the ammonia features, too.

We also conducted irradiation experiments with crystalline ammonia samples. Figure 2 displays the infrared absorption spectra of cubic crystalline ammonia before and after the irradiation at 10,
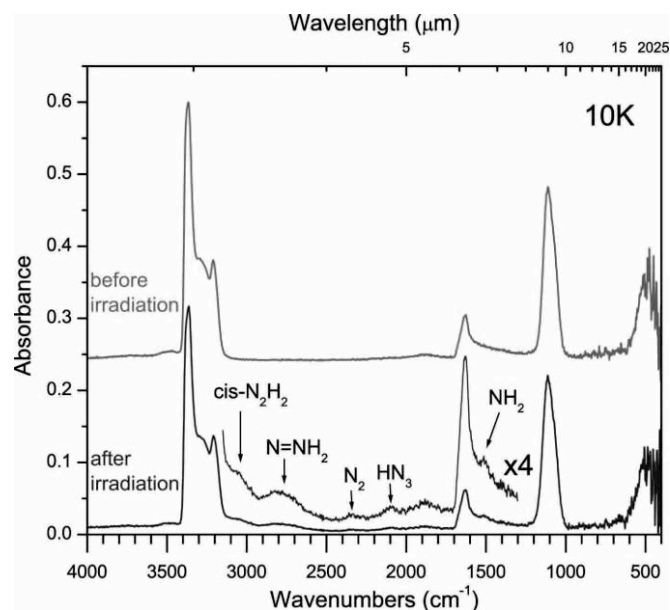

Fig. 1.—Infrared spectra of amorphous solid ammonia before and after the irradiation. [*See the electronic edition of the Journal for a color version of this figure.*]

40, and 60 K. In the case of cubic crystalline ammonia, the irradiation generated fewer novel absorption features compared to amorphous ammonia. A comparison of the spectra before and after the electron exposure shows that the spectrum at 10 K (Fig. 2a) is very similar to amorphous ammonia (Fig. 1). At 40 K (Fig. 2b), the infrared spectrum of crystalline ammonia changed slightly after irradiation. In the 60 K experiment (Fig. 2c), the spectra before and after the irradiation are almost identical. These spectra alone indicate that crystalline ammonia was converted to an amorphous sample when it was irradiated at low temperature (10 K). This amorphization process is also temperature dependent; as a matter of fact, it is less pronounced at higher temperatures of 40 and 60 K. This is similar to the amorphization of crystalline water ice by irradiation (Strazzulla et al. 1992; Mastrapa & Brown 2006). We are not able to identify the absorption features of hydrazine during the irradiation of amorphous and crystalline ammonia, since the fundamentals of hydrazine overlapped with the absorption features of ammonia. The absorption features of hydrazine showed up during the warming up phase after ammonia has sublimed. Figure 3 shows typical infrared spectra at 140, 169, and 190 K after the sublimation of ammonia is complete. Aside from the absorption features of hydrazine, we also observed a peak at 2023 cm^{-1}. That peak is most likely due to the formation of AgN$_3$ on the silver substrate, similar to that observed on the gold surface (Carlo et al. 2001). At 190 K, all reactants and products sublimed or decomposed. In the experiments of amorphous and crystalline, these results are similar. The assignments of those features are summarized in Table 1.

Another important issue is the crystallization of ammonia during the warming up phase. We conducted previously an infrared spectroscopy study of the crystallization of solid ammonia (Zheng & Kaiser 2007). It has been found that the amorphous-crystalline change in pure ammonia happens at 57 K. In this work, we monitored the change of the infrared spectra during the warming up of the irradiated samples. In postirradiation amorphous ammonia, the transition from the amorphous to the crystalline structure started at 66 K and was completed at about 75 K. This took 20 minutes under identical conditions compared to 4 minutes for

TABLE 1
Infrared Absorption Features of the Newly Formed Species in Solid Ammonia

Absorption (cm^{-1})	Literature Value (cm^{-1})	Ref.	Assignment	
			Species	Feature
During Irradiation				
1514..	1499	1	$\bullet NH_2$	Bend
2088..	2140	2	HN_3	N—N—N asym. stretch
	2043–2076	3	$NH_4^+N_3^-$	N—N—N asym. stretch
2348..	2374	4	N_2	N≡N stretch
2805..	2805	5	$N=NH_2$	N—H stretch
3052..	3066	4	cis-HN=NH	ν_1 N—H sym. stretch
During Warming				
890..	884	6	N_2H_4	ν_6 NH_2 rock
1072..	1066	6	N_2H_4	ν_{12} NH_2 rock
1136..	1126	6	N_2H_4	ν_5 N—N stretch
1606..	1603	6	N_2H_4	ν_3 NH_2 deformation
2023..	2030	7	AgN_3	N—N—N asym. stretch
2980..	2963	4	cis-HN=NH	ν_5 N—H asym. stretch
3194..	3200	6	N_2H_4	ν_2 NH_2 sym. stretch
3300..	3310	6	N_2H_4	$\nu_1 NH_2$ asym. stretch
3319..	3310	6	N_2H_4	ν_8 NH_2 asym. stretch

References.—(1) Milligan & Jacox 1965; (2) Shimanouchi 1977; (3) Carlo et al. 2001; (4) our theoretical calculations (the detailed structures and frequencies are available from the authors on request); (5) Sylwester & Dervan 1984, Teles et al. 1989; (6) Durig et al. 1966; (7) Dows et al. 1955, Porezag et al. 2000, Carlo et al. 2001.

the nonirradiated sample. In the case of the postirradiation crystalline ammonia sample, which has been amorphized during the irradiation, the change to a crystalline sample started at about 60 K and was completed at 70 K. In both cases, the transition to the crystalline phase in the postirradiation samples occurs at higher temperature than in the nonirradiated, pure ammonia. As we reported (Zheng & Kaiser 2007), a comixture of 1% of water (H_2O) into pure ammonia increased the amorphous-crystalline transition temperature from 57 to 65 K. Based on our results of the irradiated ammonia samples, hydrazine probably has the same effect, and hydrazine generated by the electron exposure delayed the crystallization point to 66 K. Our mass spectral results (see below) showed that more hydrazine was produced in amorphous ammonia. That can explain why the irradiated, amorphous sample has a higher transition temperature. From the infrared spectra, we can also see that the absolute formation of new cis-HN=NH and $N=NH_2$ products is enhanced in the amorphous ammonia sample compared to the crystalline ice (Table 2).

3.2. Mass Spectra

We monitored the species released into the gas phase with a quadrupole mass spectrometer during irradiation and after irradiation. During the irradiation, the pressure in the main chamber was about $(6-9) \times 10^{-11}$ torr, and the species released into the gas phase are below the detection limit of our mass spectrometer. After the irradiation, the samples were held at a constant temperature for 1 hr and warmed up at the speed of 0.5 K minute^{-1}. The mass spectral results demonstrate that H_2, N_2H_4, and N_2 were released. Figure 4 presents mass spectral results during the warming up of the amorphous ammonia. In the blank experiment (Fig. 4a), the sublimation of ammonia started at about 80 K and was complete at 110 K. Two H_2^+ ($m/z = 2$) peaks were detected between 10 and 30 K, centered at 17 and 23 K, respectively. A third, broad peak of H_2^+ ($m/z = 2$) was observed between 85 and 115 K. Furthermore, a broad peak at $m/z = 28$ (N_2^+) is detectable at 90–115 K. Since the profiles of $m/z = 2$

(third peak) and of $m/z = 28$ are similar to the profile of the parent peak of ammonia, it is likely that $m/z = 2$ and $m/z = 28$ result from dissociative ionization of the ammonia parent and ion-molecule reactions in the electron impact ionizer. In addition, a very small signal at $m/z = 32$ has been observed at 100–110 K. That probably is due to the tiny amount of molecular oxygen in the ammonia gas. Its effect in the experiments can be ignored, because the intensities of the mass spectra show that the amount of molecular oxygen in our ammonia samples is below 50 ppm. In the irradiation experiment (Fig. 4b), two extra H_2 peaks showed up between 66 and 75 K, centered at 69.5 and 71.0 K, respectively. The broad peaks of H_2^+ ($m/z = 2$) also showed up between 85 and 115 K. This signal can be contributed by the newly formed molecular hydrogen during the irradiation of the ammonia sample. Similar to molecular hydrogen, two extra peaks of molecular nitrogen monitored via its molecular ion at $m/z = 28$ appear. Most importantly, ion counts of hydrazine (N_2H_4) were detected via its parent ion at $m/z = 32$ between 140 and 185 K. We observed two maxima during the sublimation in the mass spectra of N_2H_4 at 158 and 173 K. This may indicate that N_2H_4 has two tautomers (trans- or cis-configuration; Liu & Giguere 1952) interacting with the silver substrate distinctively. We also noticed that the sublimation of ammonia has been delayed compared to the nonirradiated sample. The ammonia peak is broader than that in the blank experiment and shows a shoulder at 109 K. Ammonia sublimed earlier than hydrazine. However, some ammonia molecules could be trapped in hydrazine.

We would like to compare these results now with those obtained from the crystalline ammonia samples. Figure 5 shows the ion currents during the warming up of cubic crystalline ammonia. Fig. 5a is from the blank experiment. Figures 5b, 5c, and 5d are from the irradiation experiments conducted at 10, 40, and 60 K, respectively. For the experiment carried out at 10 K (Fig. 5b), the new molecular hydrogen peaks are centered at 63 and 67 K. Their positions differ from those in the amorphous ammonia sample (Fig. 4b); their intensities are also much lower. Because
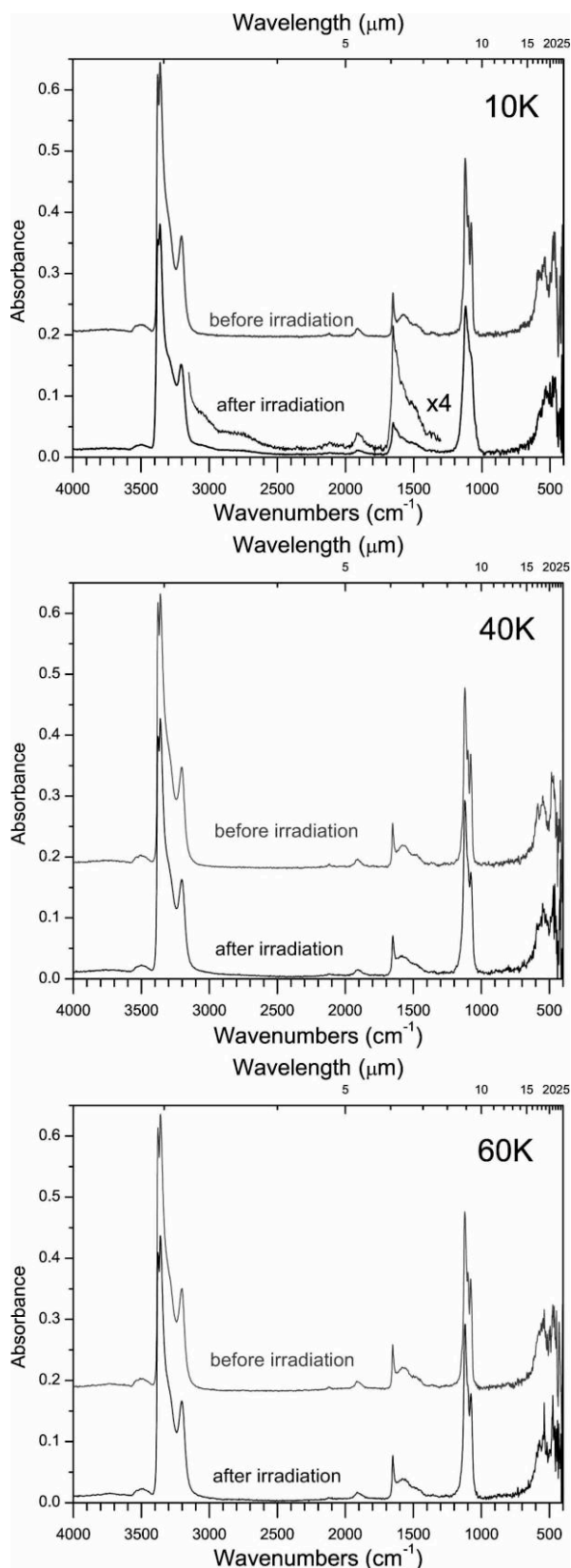
FIG. 2.—Infrared spectra of cubic crystalline solid ammonia before and after the irradiation. [*See the electronic edition of the Journal for a color version of this figure.*]
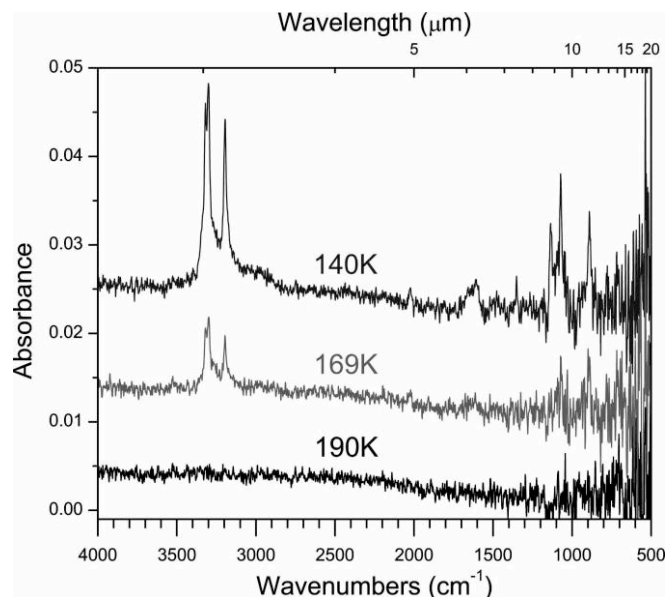

FIG. 3.—Infrared spectra of the postirradiation sample taken in the warm-up phase. [*See the electronic edition of the Journal for a color version of this figure.*]

of the lower intensity, the only new peak of the molecular nitrogen ion was observed at 67 K. These novel peaks of molecular hydrogen and nitrogen have not been observed in experiments conducted at 40 and at 60 K. The remaining features are similar to the experiment of amorphous ammonia such as the hydrazine produced via the irradiation, which is released between 140 and 185 K.

Aside from the observation of molecular hydrogen (H$_2$), molecular nitrogen (N$_2$), and hydrazine (N$_2$H$_4$), we have also detected ion counts at $m/z = 31$, 30, and 29, corresponding to N$_2$H$_3^+$, N$_2$H$_2^+$, and N$_2$H$^+$, respectively. Figure 6 presents the evolution of the ion counts of those species versus the temperature. For comparison, the ion profile of N$_2$H$_4$ at $m/z = 32$ is also plotted. The profile of $m/z = 31$ is identical to the one of the molecular ion of N$_2$H$_4$, but its intensity is much lower. So it is an ionization fragment of N$_2$H$_4$ generated in the mass spectrometer ionizer, i.e., N$_2$H$_3^+$. N$_2$H$_4$ can also undergo dissociative ionization to give N$_2$H$_2^+$ and N$_2$H$^+$. Therefore, a part of the ion counts at $m/z = 30$ and 29 is expected to originate from the hydrazine. However, the signal of $m/z = 30$ and 29 could still be observed after hydrazine has sublimed. That might imply that some N$_2$H$_2$ molecules were bonded to the surface of the silver substrate. Since N$_2$H$_2$ is not stable at elevated temperatures (Biehl & Stuhl

TABLE 2
PEAK AREAS OF THE INFRARED ABSORPTIONS OF THE NEWLY FORMED SPECIES IN AMORPHOUS AND CRYSTALLINE AMMONIA ICES AFTER THE IRRADIATION

	PEAK POSITION	PEAK AREA (cm^{-1})	
SPECIES	(cm^{-1})	Amorphous (10 K)	Crystalline (10 K)
cis-HN=NH	3052	0.43 ± 0.09	0.15 ± 0.03
N=NH$_2$	2805	0.88 ± 0.18	0.56 ± 0.11
N$_2$	2348	0.11 ± 0.03	. . .[a]
N=N=NH...........	2088	0.19 ± 0.04	. . .[a]
NH$_2$	1514	0.23 ± 0.05	. . .[a]
N$_2$H$_4$ [b]	3194	0.46 ± 0.09	0.38 ± 0.08

[a] Value is lower than the detection limit.
[b] The intensity of N$_2$H$_4$ peak was measured at 140 K when all ammonia is sublimed.
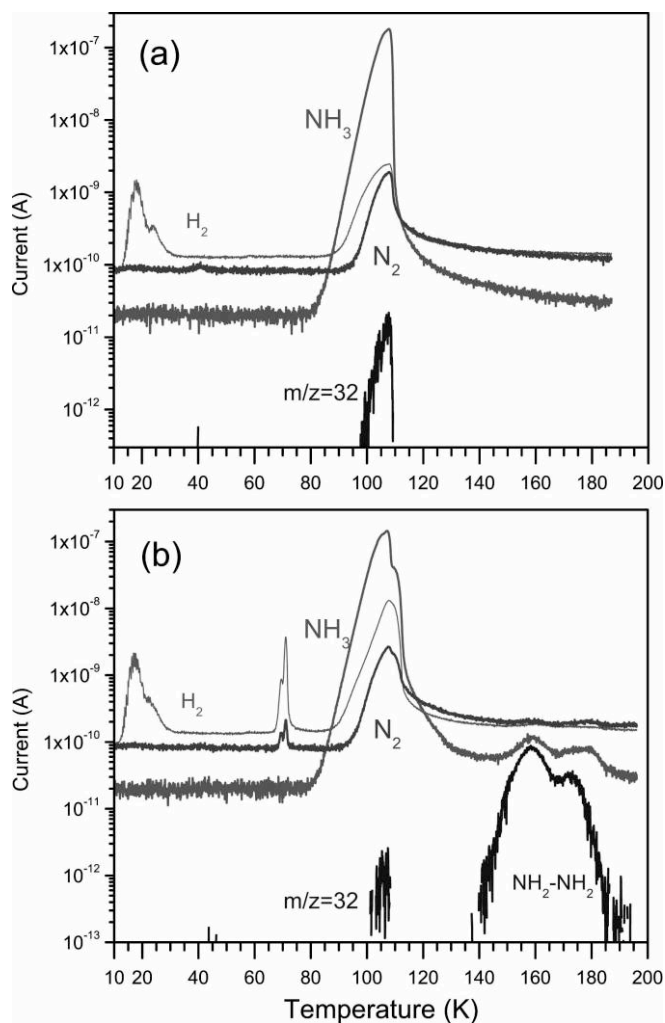
Fig. 4.— Temporal evolution of the ion currents of molecular hydrogen (H_2), molecular nitrogen (N_2), hydrazine (N_2H_4), and ammonia (NH_3) during the warm-up phase of 10 K irradiated amorphous ammonia. (*a*) 0 nA; (*b*) 100 nA. [*See the electronic edition of the Journal for a color version of this figure.*]

Fig. 5.— Temporal evolution of the ion currents of molecular hydrogen (H_2), molecular nitrogen (N_2), hydrazine (N_2H_4), and ammonia (NH_3) during the warm-up phase of irradiated cubic crystalline ammonia. (*a*) 0 nA (no irradiation), (*b*) 100 nA, irradiated at 10 K, (*c*) 100 nA, irradiated at 40 K, and (*d*) 100 nA, irradiated at 60 K. [*See the electronic edition of the Journal for a color version of this figure.*]

1994), the intensity of its fragment NNH^+ was higher than that of the parent molecule. Although HN_3 has been detected in the condensed phase at 10 K with infrared spectroscopy, it has not been detected via mass spectrometry, because it easily decomposed during the warm up. Note that from the temporal evolution of the ion currents, we observed that the positions of the newly formed molecular hydrogen peaks are correlated to the phase transition in the solid ammonia. In the case of postirradiated, amorphous ammonia, the phase transition started at 66 K and was complete at about 75 K. The hydrogen molecules were released between 66 and 75 K. For the postirradiation crystalline ammonia in the 10 K experiment, the phase transition started at about 60 K; it has been finalized at 70 K.

In order to compare the production rates of the newly formed molecules at different temperatures and amorphous versus crystalline samples, the ion currents of the newly formed H_2, N_2, and N_2H_4 molecules were integrated and, accounting for the pumping speed and molecular masses, converted to the number of molecules synthesized N (Zheng et al. 2006a). The data are summarized in Table 3. The details of mass spectrometer calibration can be found in Kaiser et al. (1995) and Zheng et al. (2006a). We estimated the effective pumping speeds for H_2, N_2, and N_2H_4 in our experiments to be 604, 760, and 686 L s^{-1}, respectively. The
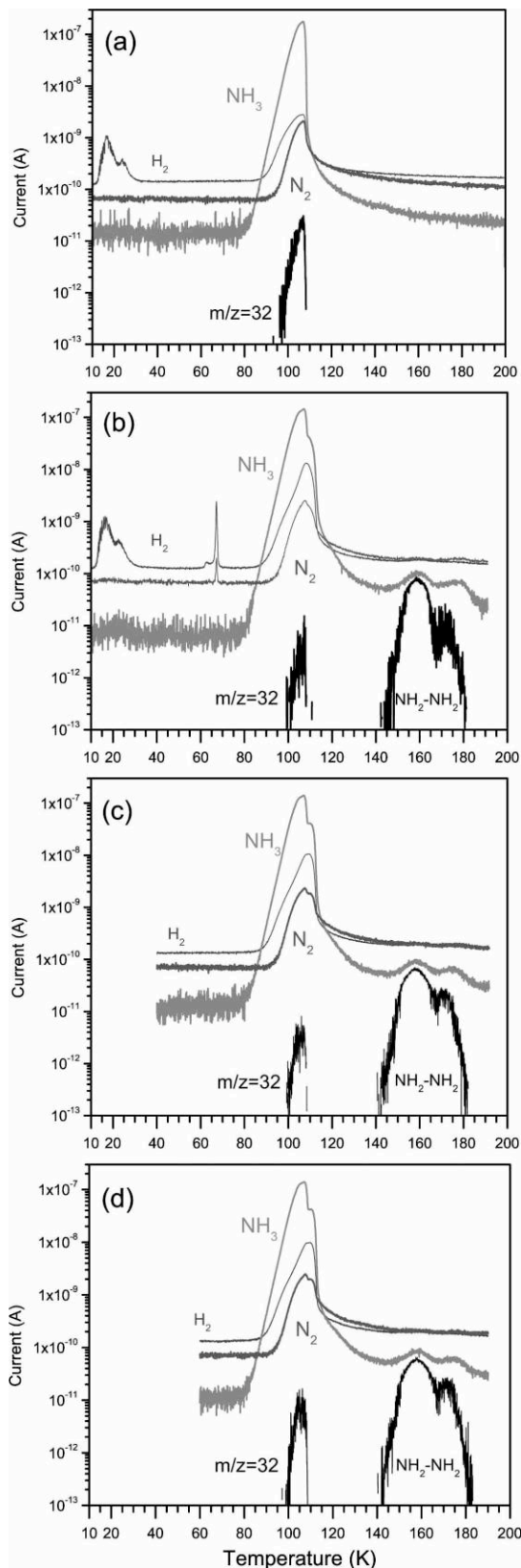
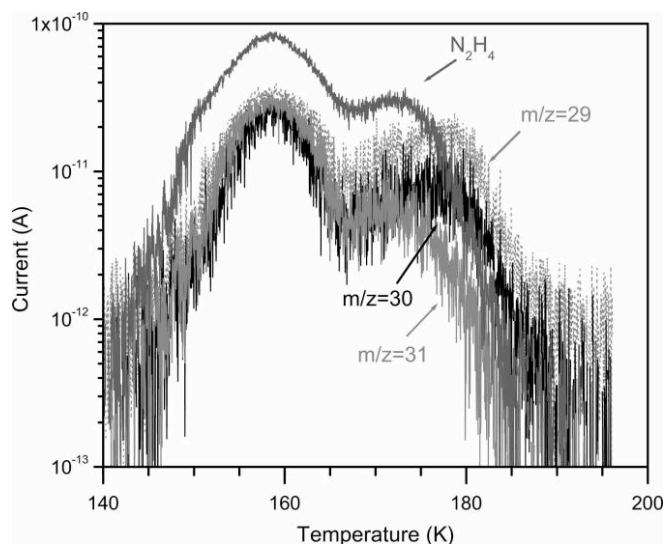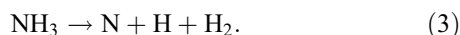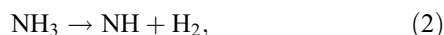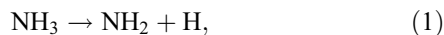Fig. 6.—Ion currents of mass $m/z = 31$, 30, and 29 during the warming up of the postirradiated ammonia; $m/z = 31$, 30, and 29 correspond to N$_2$H$_3^+$, N$_2$H$_2^+$, and N$_2$H$^+$, respectively. [*See the electronic edition of the Journal for a color version of this figure.*]

TABLE 3

Number of Molecular Hydrogen (H$_2$), Nitrogen (N$_2$), and Hydrazine (N$_2$H$_4$) Molecules Produced in Amorphous and Cubic Crystalline Solid Ammonia by Electron Irradiation

	Amorphous	Crystalline		
Molecule	10 K	10 K	40 K	60 K
H$_2$	6.4×10^{16}	5.8×10^{16}	5.0×10^{16}	4.6×10^{16}
N$_2$	3.1×10^{16}	1.9×10^{16}	2.1×10^{16}	2.4×10^{16}
N$_2$H$_4$	$>3.7 \times 10^{15}$	$>2.5 \times 10^{15}$	$>2.7 \times 10^{15}$	$>2.5 \times 10^{15}$

Note.—The uncertainties of the values are about $\pm 30\%$.

troscopically, since all of its fundamentals overlapped with the absorptions of the ammonium sample,

$$2NH_2 \rightarrow [N_2H_4]^*, \tag{4}$$

$$[N_2H_4]^* \rightarrow N_2H_4, \tag{5a}$$

$$[N_2H_4]^* \rightarrow N_2H_3 + H, \tag{5b}$$

$$[N_2H_4]^* \rightarrow N_2H_2/NNH_2 + H_2. \tag{5c}$$

The proposed formation of the N$_2$H$_2$ isomers cis-diazene (cis-HN=NH) and iso-diazene (N=NH$_2$) via reaction (5c) would result in pseudo first-order kinetics of their formation following the temporal evolution via equation (6), where t is the irradiation time, a is a constant, and k is the rate constant of the unimolecular decomposition process from the internally excited hydrazine molecule. As a matter of fact, the temporal profile of the integrated absorption profiles of both N$_2$H$_2$ isomers during the irradiation of the ammonia sample could be fit with pseudo first-order kinetics (Fig. 7). These fits yield for cis-diazene (cis-HN=NH), $a = 0.45 \pm 0.09$ cm^{-1}, $k = 7.7 \pm 1.5 \times 10^{-4}$ s^{-1}, and for diazene (N=NH$_2$), $a = 0.88 \pm 0.18$ cm^{-1}, $k = 1.1 \pm 0.2 \times 10^{-3}$ s^{-1}. Finally, we should mention that transdiazene probably also exists, but its absorption features could be hidden under the ammonia bands. Note that this reaction sequence and the initial decomposition of ammonia via reaction (1) can also lead to hydrogen atoms which can recombine to form molecular hydrogen through reaction (7),

$$[N_2H_2](t) = a(1 - e^{-kt}), \tag{6}$$

$$H + H \rightarrow H_2. \tag{7}$$
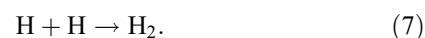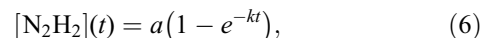
The formation of molecular nitrogen via recombination of two nitrogen atoms is very low due to the diminished concentration of nitrogen atoms in the sample. It has been suggested (Back 1984) that molecular nitrogen might be synthesized via the Rice-Herzfeld chain (reactions [8a]–[8d]). This reaction sequence could also produce radical intermediates and N$_2$H$_2$. The pseudo first-order kinetics of N$_2$H$_2$ isomers in Figure 7 is probably due to the combination of reactions (8a)–(8d) and some other reactions,

$$H + N_2H_4 \rightarrow N_2H_3 + H_2, \tag{8a}$$

$$N_2H_3 \rightarrow N_2H_2 + H, \tag{8b}$$

$$H + N_2H_2 \rightarrow N_2H + H_2, \tag{8c}$$

$$N_2H \rightarrow N_2 + H. \tag{8d}$$

pumping speed for N$_2$H$_4$ is a minimum value, because it can also be condensed on the second stage of the cold head. For the amorphous and crystalline ammonia irradiated at 10 K, the amount of hydrazine and molecular nitrogen generated in the amorphous ammonia is about 50% more than that in crystalline ammonia. Comparison of the crystalline ammonia irradiated at 10, 40, and 60 K shows that the amount of hydrazine produced at these temperatures is about the same.

4. DISCUSSION

Our experiment results clearly show that molecular hydrogen (H$_2$), molecular nitrogen (N$_2$), two N$_2$H$_2$ isomers, amino radical (NH$_2$), hydrogen azide/ammonium azide (HNNN/NH$_4$N$_3$), and hydrazine (N$_2$H$_4$) were generated in solid ammonia during the electron irradiation. We would like to address now the question of how these species were actually formed. Following interaction with an electron, an ammonia molecule can undergo unimolecular decomposition to form a hydrogen atom and an amino radical (reaction [1]). The spin-forbidden dissociation to form the NH radical and molecular hydrogen via reaction (2) can be expected to be less likely. Similarly, the simultaneous rupture of three nitrogen–hydrogen bonds to form atomic nitrogen holds a very low probability (reaction [3]). Therefore, we propose that a unimolecular decomposition of ammonia via reaction (1) presents the initial step,
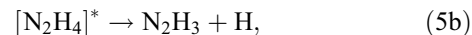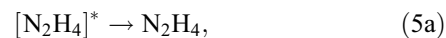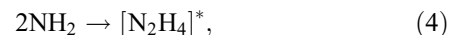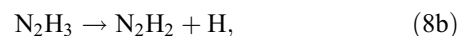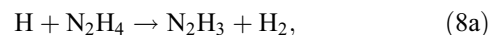
$$NH_3 \rightarrow NH_2 + H, \tag{1}$$

$$NH_3 \rightarrow NH + H_2, \tag{2}$$

$$NH_3 \rightarrow N + H + H_2. \tag{3}$$

Two *neighboring* amino radicals can recombine to form internally excited hydrazine, [N$_2$H$_4$]*, via reaction (4). We propose that the internally excited hydrazine molecule can either be stabilized to hydrazine (reaction [5a]) or undergo unimolecular decomposition to form the N$_2$H$_3$ radical plus atomic hydrogen and the observed N$_2$H$_2$ isomers NNH$_2$ and HNNH (reactions [5b]/[5c]). Recall that the N$_2$H$_3$ radical could not be detected spec-
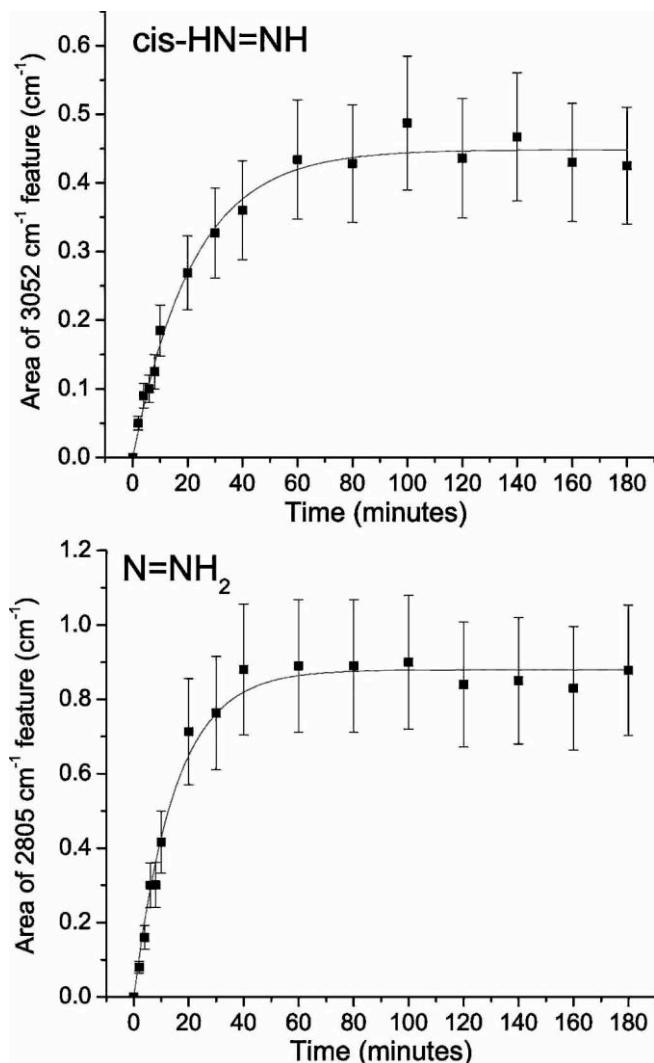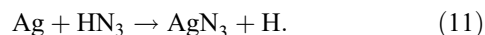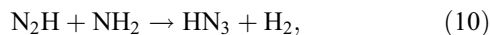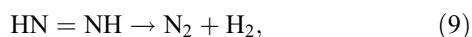
Fig. 7.—Intensities (in units of the integrated peak area) of cis-diazene (cis-HN=NH) and iso-diazene (N=NH$_2$) absorption features during the irradiation.

Note that N$_2$H$_2$ is very unstable. Experimental measurements show that N$_2$H$_2$ is about 210 kJ mol^{-1} higher in energy than the separated molecular nitrogen and molecular hydrogen products (Biehl & Stuhl 1994). Theoretical calculations indicate that cis-diazene lies 22 kJ mol^{-1} above transdiazene; isodiazene was found to be 101 kJ mol^{-1} higher in energy than transdiazene (Biczysko et al. 2006). Therefore, a N$_2$H$_2$ molecule may decompose to produce molecular nitrogen and hydrogen (reaction [9]) if the warming phase supplies sufficient energy; likewise, a small fraction of molecular nitrogen might arise from unimolecular decomposition of the N$_2$H$_2$ during the electron irradiation. Finally, the formation route to HN$_3$ is a tricky issue. Because of its low abundance, we failed to plot the temporal profile of its absorption during the irradiation. Therefore, it is not feasible to extract the kinetics and, hence, likely rate laws. The major fraction of HN$_3$ was probably formed through the reaction between N$_2$H and NH$_2$ radicals (reaction [10]), since the concentration of NH$_2$ is relatively high, and N$_2$H is also available from reaction (8c). HN$_3$ molecules' contact with silver substrate can undergo reaction (11) to form AgN$_3$. The interaction of HN$_3$ and NH$_3$ can give NH$_4^+$N$_3^-$; recall that the latter might also be a viable candidate for the 2088 cm^{-1} absorption band,

$$HN = NH \rightarrow N_2 + H_2, \qquad (9)$$

$$N_2H + NH_2 \rightarrow HN_3 + H_2, \qquad (10)$$

$$Ag + HN_3 \rightarrow AgN_3 + H. \qquad (11)$$

Since water (H$_2$O), ammonia (NH$_3$), and methane (CH$_4$) are important hydrogen-containing molecules in the solar system and in the interstellar medium, it will be interesting to compare the irradiation effects of those three species under identical experimental conditions such as temperature and electron energy, as conducted in our laboratory. The major reaction steps are similar among them. A comparison of both the water (Zheng et al. 2006a) and methane (Bennett et al. 2006) with the ammonia system suggests that the first step following the electron irradiation is the unimolecular decomposition of the water, ammonia, and methane molecule via O—H, N—H, and C—H bond ruptures to produce a hydrogen atom plus a radical (OH, NH$_2$, and CH$_3$). The hydrogen atom and the corresponding radical can "recycle" the parent molecule again. In addition, two hydrogen atoms can combine to form molecular hydrogen. Most importantly, if the generated radicals are in close proximity to a second radical (neighboring radicals), two radicals can recombine, yielding internally excited H$_2$O$_2$ (water system), N$_2$H$_4$ (hydrazine system), and C$_2$H$_6$ (methane system). These molecules can either be stabilized by the surrounding matrix or undergo unimolecular decomposition via atomic and molecular hydrogen loss pathways. For example, considering the stability of internally excited H$_2$O$_2$, N$_2$H$_4$, and C$_2$H$_6$, the least stable molecule is H$_2$O$_2$; C$_2$H$_6$ presents the most stable species. In water ice, molecular oxygen is formed from a precursor such as H$_2$O$_2$ (Laffon et al. 2006). The formation of molecular nitrogen in solid ammonia could be via N$_2$H$_4$ through the Rice-Herzfeld chain. In the solid methane, the newly generated C$_2$H$_6$ can decompose to produce an ethyl radical (C$_2$H$_5$) and ethylene (C$_2$H$_4$); acetylene (C$_2$H$_2$) can be formed only via multiple steps involving a radiolysis of ethylene.
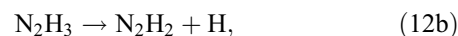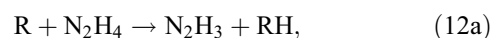
Finally, we would like to address briefly the effect of the ice morphology (crystalline vs. amorphous) on the formation of the reaction products quantitatively. In electron-irradiated water ice, we found that the production rate of hydrogen peroxide (H$_2$O$_2$) in amorphous water ice is higher than in crystalline water ice samples (Zheng et al. 2007). In the present study of solid ammonia, the production of hydrazine (N$_2$H$_4$) was also found to be enhanced in the amorphous sample. On the other hand, there is a striking difference. The production of hydrogen peroxide (H$_2$O$_2$) in irradiated crystalline water ice is strongly temperature dependent (Moore & Hudson 2000; Gomis et al. 2004; Zheng et al. 2006b); however, the formation of hydrazine (N$_2$H$_4$) in the irradiated crystalline ammonia does not show any temperature dependence. How can this be explained? The production of hydrogen peroxide (H$_2$O$_2$) is affected by the diffusion of atoms (H) and radicals (OH) in irradiated water ice. The decrease of the hydrogen peroxide production in water ice at higher temperature was found to be due to the recombination of mobile hydrogen atoms with hydroxyl radicals in the matrix cage to "recycle" water molecules. In solid ammonia, only one-third of the hydrogen atoms take part in hydrogen bonds, because each ammonia molecule has only one lone pair of electrons. The hydrogen bond between the ammonia molecules is weaker than between two water molecules (13 kJ mol^{-1} vs. 21 kJ mol^{-1}; Jeffrey 1997). Because of the weaker interactions between the molecules in solid ammonia, the newly formed hydrogen atoms may be able to escape the matrix cage more efficiently to react with a second hydrogen atom to form molecular hydrogen. Based on our results, we suggest that the temperature dependence of this process in solid ammonia is not as strong as in water ice.

5. ASTROPHYSICAL IMPLICATIONS

It has been reported that the fraction of molecular nitrogen in a dark cloud is very low. Maret et al. (2006) estimated that the abundance of molecular nitrogen with respect to water is only about 1% in the grain mantles in the B68 prestellar core. Their models indicate that the main nitrogen reservoir is ammonia ice with an abundance of 7% with respect to water. In comets, the N$_2$ abundance is also minor (<0.03% with respect to water; Cochran et al. 2000; Iro et al. 2003). It has been suggested that comets might be aggregates of interstellar dust grains that survived the formation of the solar nebula (Irvine et al. 2000). Therefore, ammonia could also be the main source of nitrogen in comets. Based on our experiments, an interaction of ammonia with ionizing radiation can ultimately produce molecular nitrogen. So, it is expected that the ammonia on various solar system objects, either neat or mixed with water, is expected to decrease over the exposure time, whereas the fraction of molecular nitrogen would be enhanced. This is in agreement with previous work. For example, Lanzerotti et al. (1984) suggested that the bombardment of magnetosphere ions might cause the depletion of ammonia on the Saturnian satellite surfaces. Very recently, Loeffler et al. (2006) investigated the irradiation of water-ammonia ice mixture with 100 keV protons. They recommended that the unexpected emission of plumes of water vapor and nitrogen on Saturn's icy moon Enceladus probably is due to the radiolytic decomposition of ammonia. Enceladus is believed to be a dominant nitrogen source in Saturn's magnetosphere (Waite et al. 2006; Smith et al. 2007). It has been suggested that the N$^+$ signal detected by the *Cassini Plasma Spectrometer* (*CAPS*) may originate from N$_2$ instead of ammonia, but ammonia still cannot be ruled out. It might be possible that the N$_2$ originates from NH$_3$ below the surface of Enceladus (Smith et al. 2007). Aside from the possible production of molecular nitrogen from ammonia on the Saturnian satellites, it has been suggested that sputtering of ammonia contributed to the abundance of N$_2$ on Triton and Pluto (Johnson 1998).

It is also interesting to consider the nitrogen-rich atmospheres of proto-Earth and Titan. It has been suggested that some of the water on Earth might be delivered by comets (Meier et al. 1998; Laufer et al. 1999). If that is true, then ammonia could be delivered to Earth simultaneously. Currently, the atmosphere of Earth is dominated by molecular nitrogen and oxygen, whereas the concentration of ammonia is extremely low. Consequently, ammonia must have been converted to molecular nitrogen. In this scenario, solar UV photons, the solar wind, and cosmic-ray particles could be the driving force of this process. The atmosphere of Titan, the largest moon of Saturn, is dominated by molecular nitrogen, methane, and other hydrocarbons (Barth & Toon 2006; Tobie et al. 2006; Vuitton et al. 2006). And the ice on the surface of Titan is predominantly composed of hydrocarbons (Turtle et al. 2007). The molecular nitrogen in the atmosphere of Titan could also originate from ammonia (Smythe et al. 2006) that is bombarded by energetic particles and UV photons. It is worth mentioning that the principal nitrogen-hydrogen product of the ammonia irradiation-hydrazine (N$_2$H$_4$) can undergo chain reactions with hydrocarbon radicals (R) to produce hydrocarbon and molecular nitrogen *if* the entrance barriers to these processes can be overcome (reactions [12a]–[12d]; Back 1984). Note, for instance, that the reaction rate of related radicals such as cyano (CN), which are also important transient species in Titan's atmosphere, with ethane, for instance, increases as the temperature decreases, holding a maximum rate constant on the order of 10^{-10} cm^3 s^{-1} (Sims et al. 1993; Sims & Smith 1995). Unfortunately, the rate constants of cyano radicals with hydrazine and the degradation products at low temperatures are currently unknown. If these rate constants turn out to be at the same order of magnitude as those of the reactions with ethane, the production of molecular nitrogen from hydrazine may be even very efficient at very low temperatures as present in Titan's atmosphere. Since hydrazine (N$_2$H$_4$) is an important product from the irradiation of ammonia and hydrocarbon and cyano radicals can be produced from their parent molecules via photolysis, the existence of these radicals may actually help to speed up the processes of molecular nitrogen production in Titan's atmosphere,

$$R + N_2H_4 \rightarrow N_2H_3 + RH, \tag{12a}$$

$$N_2H_3 \rightarrow N_2H_2 + H, \tag{12b}$$

$$R + N_2H_2 \rightarrow N_2H + RH, \tag{12c}$$

$$N_2H \rightarrow N_2 + H. \tag{12d}$$

REFERENCES

Atreya, S. K., Mahaffy, P. R., Niemann, H. B., Wong, M. H., & Owen, T. C. 2003, Planet. Space Sci., 51, 105
Back, R. A. 1984, Rev. Chem. Intermediates, 5, 293
Barth, E. L., & Toon, O. B. 2006, Icarus, 182, 230
Bauer, J. M., Roush, T. L., Geballe, T. R., Meech, K. J., Owen, T. C., Vacca, W. D., Rayner, J. T., & Jim, K. T. C. 2002, Icarus, 158, 178
Bennett, C. J., Jamieson, C. S., Mebel, A. M., & Kaiser, R. I. 2004, Phys. Chem. Chem. Phys., 6, 735
Bennett, C. J., Jamieson, C. S., Osamura, Y., & Kaiser, R. I. 2006, ApJ, 653, 792
Biczysko, M., Poveda, L. A., & Varandas, A. J. C. 2006, Chem. Phys. Lett., 424, 46
Biehl, H., & Stuhl, F. 1994, J. Chem. Phys., 100, 141
Carlo, S. R., Torres, J., & Fairbrother, D. H. 2001, J. Phys. Chem. B, 105, 6148
Catalano, E., Sanborn, R. H., & Frazer, J. W. 1963, J. Chem. Phys., 38, 2265
Cecchi-Pestellini, C., Aiello, S., & Barsella, B. 1995, MNRAS, 274, 134
Cesarsky, C. J., & Volk, H. J. 1978, A&A, 70, 367
Clayton, D. D., & Jin, L. 1995, ApJ, 451, 681
Cochran, A. L., Cochran, W. D., & Barker, E. S. 2000, Icarus, 146, 583
Cooper, J. F., Christian, E. R., Richardson, J. D., & Wang, C. 2003, Earth Moon Planets, 92, 261

Cooper, J. F., Johnson, R. E., Mauk, B. H., Garrett, H. B., & Gehrels, N. 2001, Icarus, 149, 133
De Vries, A. E., Haring, R. A., Haring, A., Klein, F. S., Kummel, A. C., & Saris, F. W. 1984, J. Phys. Chem., 88, 4510
Dows, D. A., Whittle, E., & Pimentel, G. C. 1955, J. Chem. Phys., 23, 1474
Durig, J. R., Bush, S. F., & Mercer, E. E. 1966, J. Chem. Phys., 44, 4238
Durig, J. R., & Zheng, C. 2002, Vibrational Spectrosc., 30, 59
Emery, J. P., Burr, D. M., Cruikshank, D. P., Brown, R. H., & Dalton, J. B. 2005, A&A, 435, 353
Farenzena, L. S., et al. 2005, Earth Moon Planets, 97, 311
Gerakines, P. A., Schutte, W. A., & Ehrenfreund, P. 1996, A&A, 312, 289
Gomis, O., Leto, G., & Strazzulla, G. 2004, A&A, 420, 405
Greenberg, J. M., van de Bult, C. E. P. M., & Allamandola, L. J. 1983, J. Phys. Chem., 87, 4243
Haring, R. A., Haring, A., Klein, F. S., Kummel, A. C., & De Vries, A. E. 1983, Nucl. Instrum. Methods Phys. Res., 211, 529
Hofstadter, M. D., & Muhleman, D. O. 1989, Icarus, 81, 396
Hwang, D. Y., & Mebel, A. M. 2003, J. Phys. Chem. A, 107, 2865
Iro, N., Gautier, D., Hersant, F., Bockelée-Morvan, D., & Lunine, J. I. 2003, Icarus, 161, 511

Irvine, W. M., Schloerb, F. P., Crovisier, J., Fegley, B., Jr., & Mumma, M. J. 2000, in Protostars and Planets IV, ed. V. Mannigs, A. P. Boss, & S. S. Russell (Tucson: Univ. Arizona Press), 1159

Jeffrey, G. A. 1997, An Introduction to Hydrogen Bonding (New York: Oxford Univ. Press)

Jewitt, D. C., & Luu, J. 2004, Nature, 432, 731

Johnson, R. E. 1998 in Solar System Ices (Dordrecht: Kluwer), 303

Johnson, R. E., Lanzerotti, L. J., Brown, W. L., Augustyniak, W. M., & Mussil, C. 1983, A&A, 123, 343

Kaiser, R. I., Jansen, P., Petersen, K., & Roessler, K. 1995, Rev. Sci. Instrum., 66, 5226

Laffon, C., Lacombe, S., Bournel, F., & Parent, P. 2006, J. Chem. Phys., 125, 204714

Lanzerotti, L. J., Brown, W. L., Marcantonio, K. J., & Johnson, R. E. 1984, Nature, 312, 139

Laufer, D., Notesco, G., Bar-Nun, A., & Owen, T. 1999, Icarus, 140, 446

Lindal, G. F. 1992, AJ, 103, 967

Liu, I. D., & Giguere, P. A. 1952, J. Chem. Phys., 20, 136

Loeffler, M. J., Raut, U., & Baragiola, R. A. 2006, ApJ, 649, L133

Maret, S., Bergin, E. A., & Lada, C. J. 2006, Nature, 442, 425

Mastrapa, R. M. E., & Brown, R. H. 2006, Icarus, 183, 207

Matus, M. H., Arduengo, A. J., & Dixon, D. A. 2006, J. Phys. Chem. A, 110, 10116

Meier, R., Owen, T. C., Matthews, H. E., Jewitt, D. C., Bockelee-Morvan, D., Biver, N., Crovisier, J., & Gautier, D. 1998, Science, 279, 842

Milligan, D. E., & Jacox, M. E. 1965, J. Chem. Phys., 43, 4487

Moore, M. H., & Hudson, R. L. 2000, Icarus, 145, 282

Pople, J. A., & Curtiss, L. A. 1991, J. Chem. Phys., 95, 4385

Porezag, D., Pederson, M. R., & Liu, A. Y. 2000, Phys. Rev. B, 61, 13230

Rosengren, K., & Pimentel, G. C. 1965, J. Chem. Phys., 43, 507

Roush, T. L. 2001, J. Geophys. Res., 106, 33315

Shimanouchi, T. 1977, J. Phys. Chem. Ref. Data, 6, 993

Sill, G., Fink, U., & Ferraro, J. R. 1980, J. Opt. Soc. Am., 70, 724

Sims, I. R., Queffelec, J. L., Travers, D., Rowe, B. R., Herbert, L. B., Karthauser, J., & Smith, I. W. M. 1993, Chem. Phys. Lett., 211, 461

Sims, I. R., & Smith, I. W. M. 1995, Annu. Rev. Phys. Chem., 46, 109

Smith, H. T., et al. 2007, Icarus, 188, 356

Smythe, W. D., Nelson, R. M., Shirley, J. H., & Boryta, M. C. 2006, Lunar Planet. Sci., 37, abs. 2136

Strazzulla, G., Baratta, G. A., Leto, G., & Foti, G. 1992, Europhys. Lett., 18, 517

Sylwester, A. P., & Dervan, P. B. 1984, J. Am. Chem. Soc., 106, 4648

Szulczewski, G. J., & White, J. M. 1998, Surf. Sci., 406, 194

Teles, J. H., Maier, G., Hess, B. A., & Schaad, L. J. 1989, Chem. Berichte, 122, 749

Tobie, G., Lunine, J. I., & Sotin, C. 2006, Nature, 440, 61

Turtle, E. P., Perry, J., McEwen, A. S., West, R. A., & Fussner, S. 2007, Lunar Planet. Sci., 38, abs. 2322

Vuitton, V., Yelle, R. V., & Anicich, V. G. 2006, ApJ, 647, L175

Waite, J. H., Jr., et al. 2006, Science, 311, 1419

Zheng, W., Jewitt, D., & Kaiser, R. I. 2006a, ApJ, 639, 534

———. 2006b, ApJ, 648, 753

———. 2007, Chem. Phys. Lett., 435, 289

Zheng, W., & Kaiser, R. I. 2007, Chem. Phys. Lett., 440, 229